J|A|C|S
ARTICLES
Published on Web 06/06/2002

^{57}Fe Mössbauer Isomer Shifts of Heme Protein Model Systems: Electronic Structure Calculations

Yong Zhang, Junhong Mao, and Eric Oldfield*

Contribution from the Departments of Chemistry and Biophysics, University of Illinois at Urbana−Champaign, 600 South Mathews Avenue, Urbana, Illinois 61801

Received June 28, 2001. Revised Manuscript Received April 23, 2002

Abstract: We report the results of density functional theory (DFT) calculations of the ^{57}Fe Mössbauer isomer shifts (δ_{Fe}) for a series of 24 inorganic, organometallic, and metalloprotein/metalloporphyrin model systems in $S = 0$, $^1/_2$, 1, $^3/_2$, 2, and $^5/_2$ spin states. We find an excellent correlation between calculation and experiment over the entire 2.34 mm s^{-1} range of isomer shifts: a 0.07−0.08 mm s^{-1} rms deviation between calculation and experiment (corresponding to 3−4% of the total δ_{Fe} range, depending on the functionals used) with R^2 values of 0.973 and 0.981 ($p < 0.0001$). The best results are obtained by using the hybrid exchange-correlation functional B3LYP, used previously for ^{57}Fe Mössbauer quadrupole splittings and ^{57}Fe NMR chemical shifts and chemical shielding anisotropies. The relativistically corrected value of α, α^{rel}, converges with the large basis set used in this work, but the exact values vary somewhat with the methods used: −0.253 a_0^3 mm s^{-1} (Hartree−Fock; HF); −0.316 a_0^3 mm s^{-1} (hybrid HF-DFT; B3LYP), or −0.367 a_0^3 mm s^{-1} (pure DFT; BPW91). Both normal and intermediate spin state isomer shifts are well reproduced by the calculations, as is the broad range of δ_{Fe} values: from $[Fe^{VI}O_4]^{2-}$ (−0.90 mm s^{-1} expt; −1.01 mm s^{-1} calc) to $KFe^{II}F_3$ (1.44 mm s^{-1} expt; 1.46 mm s^{-1} calc). Molecular orbital analyses of all inorganic solids as well as all organometallic and metalloporphyrin systems studied reveal that there are three major core MO contributions to $\rho^{tot}(0)$, the total charge density at the iron nucleus (and hence δ_{Fe}), that do not vary with changes in chemistry, while the valence MO contributions are highly correlated with δ_{Fe} ($R^2 = 0.915$−0.938, depending on the functionals used), and the correlation between the valence MO contributions and the total MO contribution is even better ($R^2 = 0.965$−0.976, depending on the functionals used). These results are of general interest since they demonstrate that DFT methods now enable the accurate prediction of δ_{Fe} values in inorganic, organometallic, and metalloporphyrin systems in all spin states and over a very wide range of δ_{Fe} values with a very small rms error.

Introduction

^{57}Fe Mössbauer spectroscopy is a technique widely used to investigate the structures of metalloproteins, metalloporphyrins, and model systems and is a potentially powerful tool with which to deduce both geometric and electronic structures.[1] ^{57}Fe Mössbauer spectra are typically dominated by two interactions: the quadrupole splitting, which arises from the non-spherical nuclear charge distribution in the $I^* = ^3/_2$ excited state in the presence of an electric field gradient at the ^{57}Fe nucleus, and an isomer (or chemical) shift, which arises from differences in the electron density at the nucleus between the absorber (the molecule or system of interest) and a reference compound (usually α-Fe at 300 K). This interaction is given by

$$\delta_{Fe} = E_A - E_{Fe} = \frac{2\pi}{3} Ze^2(\langle R^2\rangle^* - \langle R^2\rangle)(|\psi(0)|^2_A - |\psi(0)|^2_{Fe}) \quad (1)$$

where Z represents the atomic number of the nucleus of interest (iron) and R, R* are average nuclear radii of the ground and excited states of ^{57}Fe. Since $|\psi(0)|^2_{Fe}$ is a constant, the isomer shift (from Fe) can be written as

$$\delta_{Fe} = \alpha[\rho^{tot}(0) - c] \quad (2)$$

where α is the so-called calibration constant and $\rho^{tot}(0)$ is the computed charge density at the nucleus. Clearly, it should, in principle, be possible to compute both interactions from high-quality wave functions, and in earlier work[2−4] quantum chemical methods have been used to investigate the isomer shifts in a broad range of (small) inorganic solids, such as $K_4[Fe(CN)_6]$, $K_3[Fe(CN)_6]$, $KFeF_3$, FeF_3, and $BaFeO_4$, which cover a wide range of δ_{Fe} isomer shifts values (2.34 mm s^{-1}) and spin states ($S = 0$, $^1/_2$, 1, 2, and $^5/_2$). In other work, the metalloproteins carbonmonoxymyoglobin, carbonmonoxyhemoglobin, and the corresponding deoxyproteins have been investigated by Trau-

* To whom correspondence should be addressed. E-mail: eo@chad.scs.uiuc.edu.

(1) Debrunner, P. G. In *Iron Porphyrins*; Lever, A. B. P., Gray, H. B., Eds.; VCH Publishers: New York, 1989; Vol. 3, pp 139−234.
(2) Trautwein, A.; Harris, F. E.; Freeman, A. J.; Desclaux, J. P. *Phys. Rev. B* **1975**, *11*, 4101−4105.
(3) Reschke, R.; Trautwein, A.; Desclaux, J. P. *J. Phys. Chem. Solids* **1977**, *38*, 837−841.
(4) Nieuwpoort, W. C.; Post, D.; van Duijnen, P. Th. *Phys. Rev. B* **1978**, *17*, 91−98.

twein and co-workers.[5] However, these earlier studies on proteins did not benefit from the availability of modern high-resolution crystallographic structures, and it has been unclear just how accurately Mössbauer isomer shifts in macromolecular systems can be evaluated. In particular, there have been no comprehensive studies of the six spin states, $S = 0$, $^1/_2$, 1, $^3/_2$, 2, and $^5/_2$, found in metalloporphyrins and metalloproteins. If it were shown to be possible to accurately predict the isomer shifts in all six spin states, then this would make the isomer shift an even more valuable probe of geometric and electronic structure in these systems. For example, it could be used in structure refinement in much the same way that NMR chemical shifts can be used.[6]

In our group, we were previously confronted with a similar problem: how to evaluate ^{57}Fe nuclear magnetic resonance (NMR) chemical shifts (and chemical shift tensors) in metalloproteins and metalloporphyrins. In pioneering early work, Bühl et al. showed that Hartree−Fock (HF) methods are incapable of accurately predicting metal NMR chemical shifts for a range of metal nuclei.[7] However, Bühl then showed[8] that density functional theory (DFT) methods did permit the accurate prediction of ^{57}Fe, ^{99}Ru, and ^{103}Rh NMR chemical shifts in small organometallic complexes, at least when using so-called "hybrid" DFT methods in which a small (20%) admixture of Hartree−Fock exchange is incorporated into the exchange-correlation functional. We then used this approach to successfully predict the ^{57}Fe and ^{59}Co NMR chemical shifts (and chemical shift anisotropies) in a series of inorganic (^{59}Co) and metalloporphyrin /metalloprotein (^{57}Fe) model compounds,[9,10] and following on this success, we and others[9,11−13] also successfully used DFT methods to predict ^{57}Fe Mössbauer quadrupole splittings in a series of diamagnetic metalloporphyrins and related systems.[9,11−13] However, it remained to be seen to what extent it might be possible to use these same methods to predict ^{57}Fe Mössbauer isomer shifts in paramagnetic spin state ($S = ^1/_2$, 1, $^3/_2$, 2, and $^5/_2$) metalloporphyrins and model compounds. Fortunately, Wilkens et al.[14] recently showed that use of the hybrid exchange-correlation functional, B3LYP, also permitted the accurate calculation of spin densities (and hence NMR hyperfine shifts) in a paramagnetic system, which suggested that this approach might also be applicable to predicting δ_{Fe} values in paramagnetic materials.

In this paper, we first discuss the effects of basis set size and calculational method (HF, pure, and hybrid DFT methods) on the evaluation of isomer shifts in the four inorganic systems previously investigated by Nieuwpoort et al.,[4] $K_4[Fe(CN)_6]$ ($S = 0$), $K_3[Fe(CN)_6]$ ($S = ^1/_2$), $KFeF_3$ ($S = 2$), and FeF_3 ($S = ^5/_2$), including the effects of relativistic corrections on the determination of the coefficient α (eq 2), where a "consensus value" (based on 31 determinations) of $\alpha^{rel} = -0.267 \pm 0.115$ a_0^3 mm s^{-1} (the relativistically corrected value of α) has been obtained previously.[4,12,15−17] Second, we have investigated the evaluation of 24 isomer shifts, covering both inorganic and metalloporphyrin/metalloprotein model systems, in all six spin states covering a wide experimental range of 2.34 mm s^{-1}. Third, we have investigated how the various molecular orbitals contribute to the overall charge density at the Fe nucleus, $\rho^{tot}(0)$, and hence the experimental ^{57}Fe Mössbauer isomer shifts.

Experimental Section: Computational Methods

Electronic structure calculations were carried out by using the Gaussian-98[18] and AIM-2000 programs[19] on Silicon Graphics (Mountain View, CA) O-200, O-300, and O-2000 computers. In most cases, the structures used were based on published X-ray crystallographic structures.[4,20−31] For the other three cases, geometry-optimized structures

(5) Trautwein, A. In *Structure and Bonding*; Dunitz, J. D., Hemmerich, P., Holm, R. H., Ibers, J. A., Jørgensen, C. K., Neilands, J. B., Reinen, D., Williams, R. J. P., Eds.; Springer-Verlag: New York, 1974; pp 101−167.
(6) McMahon, M.; deDios, A. C.; Godbout, N.; Salzmann, R.; Laws, D. D.; Le, H.; Havlin, R. H.; Oldfield, E. *J. Am. Chem. Soc.* **1998**, *120*, 4784−4797.
(7) Bühl, M.; Malkina, O. L.; Malkin, V. G. *Helv. Chim. Acta* **1996**, *79*, 742−754. Bühl, M. *Chem. Eur. J.* **1999**, *5*, 3514−3522.
(8) Bühl, M. *Chem. Phys. Lett.* **1997**, *267*, 251−257. Bühl, M.; Gaemers, S.; Elsevier: J. *Chem. Eur. J.* **2000**, *6*, 3272−3280.
(9) Godbout, N.; Havlin, R.; Salzmann, R.; Debrunner, P. G.; Oldfield, E. *J. Phys. Chem. A* **1998**, *102*, 2342−2350.
(10) Godbout, N.; Oldfield, E. *J. Am. Chem. Soc.* **1997**, *119*, 8065−8069.
(11) Havlin, R. H.; Godbout, N.; Salzmann, R.; Wojdelski, M.; Arnold, W.; Schulz, C. E.; Oldfield, E. *J. Am. Chem. Soc.* **1998**, *120*, 3144−3151.
(12) Nemykin, V. N.; Kobayashi, N.; Chernii, V. Y.; Belsky, V. K. *Eur. J. Inorg. Chem.* **2001**, 733−743.
(13) Grodzicki, M.; Flint, H.; Winkler, H.; Walker, F. A.; Trautwein, A. X. *J. Phys. Chem. A* **1997**, *101*, 4202−4207.
(14) Wilkens, S. J.; Xia, B.; Weinhold, F.; Markley, J. L.; Westler, W. M. *J. Am. Chem. Soc.* **1998**, *120*, 4806−4814.
(15) (a) Walker, L. R.; Wertheim, G. K.; Jaccarino, V. *Phys. Rev. Lett.* **1961**, *6*, 98−101. (b) Gol'danskii, V. I. In *Proceedings of the Dubna Conference on the Mössbauer Effect*; Consultants Bureau Enterprises: New York, 1963. (c) Danon, J. In *Application of the Mössbauer Effect in Chemistry and Solid State Physics*; International Atomic Energy Agency: Vienna, 1966. (d) Uher, R. A.; Sorensen, R. A. *Nucl. Phys.* **1966**, *86*, 1−46. (e) Gol'danskii, V. I.; Markarov, E. F.; Stukan, R. A. *Teor. Eksp. Khim.* **1966**, *2*, 504−511. (f) Dautov, L. M.; Kaipov, D. K. *Vestn. Akad. Nauk Kaz. SSR* **1967**, *23*, 49−52. (g) Ingalls, R. *Phys. Rev.* **1967**, *155*, 157−165. (h) Simanek, E.; Sroubek, Z. *Phys. Rev.* **1967**, *163*, 275−279. (i) Simanek, E.; Wong, A. Y. C. *Phys. Rev.* **1968**, *166*, 348−349. (j) Moyzis, J. A., Jr.; Drickamer, H. G. *Phys. Rev.* **1968**, *171*, 389−392. (k) Wakoh, S.; Yamashita, J. *J. Phys. Soc. Jpn.* **1966**, *21*, 1712−1726; *J. Phys. Soc. Jpn.* **1968**, *25*, 1272−1281. (l) Pleiter, F.; Kolk, B. *Phys. Lett. B* **1971**, *34*, 296−298. (m) McNab, T. K.; Micklitz, H.; Barrett, P. H. *Phys. Rev. B* **1971**, *4*, 3787−3797. (n) Sharma, R. R.; Sharma, A. K. *Phys. Rev. Lett.* **1972**, *29*, 122−124. (o) Walch, P. F.; Ellis, D. E. *Phys. Rev. B* **1973**, *7*, 903−907. (p) Trautwein, A.; Regnard, J. R.; Harris, F. E.; Maeda, Y. *Phys. Rev. B* **1973**, *7*, 947−951. (q) Duff, K. J. *Phys. Rev. B* **1974**, *9*, 66−72. (r) Akai, H.; Blügel, S.; Zeller, R.; Dederichs, P. H. *Phys. Rev. Lett.* **1986**, *56*, 2407−2410. (s) Trautwein, A. X.; Winkler, H. *Z. Naturforsch.* **1987**, *42a*, 211−212. (t) Zhang, Q.-M.; Zhang, Y.-L.; Wang, D.-S. *Comm. Theor. Phys.* **1987**, *8*, 139−151. (u) Van der heyden, M.; Micklitz, H.; Bukshpan, S.; Langouche, G. *Phys. Rev. B* **1987**, *36*, 38−43. (v) Eriksson, O.; Svane, A. *J. Phys-Condens. Mater.* **1989**, *1*, 1589−1599. (w) Jansen, N.; Spiering, H.; Gutlich, P.; Stahl, D.; Kniep, R.; Eyert, V.; Kubler, J.; Schmidt, P. C. *Angew. Chem.* **1992**, *104*, 1632−1634. (x) Guenzburger, D.; Ellis, D. E.; Zeng, Z. *Hyperfine Interact.* **1998**, *113*, 25−36. (y) Trautwein, A.; Harris, F. E. *Theor. Chim. Acta* **1973**, *30*, 45−58.
(16) Yamada, Y.; Tominaga, T. *J. Radioanal. Nucl. Chem. Lett.* **1994**, *188*, 83. Yamada, Y.; Tominaga, T. *J. Radioanal. Nucl. Chem. Lett.* **1995**, *199*, 95. Yamada, Y.; Tominaga, T. *Radiochim. Acta* **1998**, *80*, 163−170.
(17) Yamada, Y. *J. Nucl. Radiochem. Sci.* **2000**, *1*, 75−76. Yamada, Y.; Katsumata, K. *Chem. Lett.* **2000**, 746−747.
(18) Frisch, M. J.; Trucks, G. W.; Schlegel, H. B.; Scuseria, G. E.; Robb, M. A.; Cheeseman, J. R.; Zakrzewski, V. G.; Montgomery, J. A., Jr.; Stratmann, R. E.; Burant, J. C.; Dapprich, S.; Millam, J. M.; Daniels, A. D.; Kudin, K. N.; Strain, M. C.; Farkas, O.; Tomasi, J.; Barone, V.; Cossi, M.; Cammi, R.; Mennucci, B.; Pomelli, C.; Adamo, C.; Clifford, S.; Ochterski, J.; Petersson, G. A.; Ayala, P. Y.; Cui, Q.; Morokuma, K.; Malick, D. K.; Rabuck, A. D.; Raghavachari, K.; Foresman, J. B.; Cioslowski, J.; Ortiz, J. V.; Baboul, A. G.; Stefanov, B. B.; Liu, G.; Liashenko, A.; Piskorz, P.; Komaromi, I.; Gomperts, R.; Martin, R. L.; Fox, D. J.; Keith, T.; Al-Laham, M. A.; Peng, C. Y.; Nanayakkara, A.; Challacombe, M.; Gill, P. M. W.; Johnson, B.; Chen, W.; Wong, M. W.; Andres, J. L.; Gonzalez, C.; Head-Gordon, M.; Replogle, E. S.; Pople, J. A. *Gaussian 98*, Revision A.9; Gaussian, Inc.: Pittsburgh, PA, 1998.
(19) (a) Biegler-König, F. *AIM2000*, Version 1.0; University of Applied Science, Bielefeld, Germany, 2000. (b) Bader, R. F. W. *Atoms in Molecules: A Quantum Theory*; Oxford University Press: Oxford, 1990.
(20) Salzmann, R.; McMahon, M. T.; Godbout, N.; Sanders, L. K.; Wojdelski, M.; Oldfield, E. *J. Am. Chem. Soc.* **1999**, *121*, 3818−3828.
(21) Naiyin, L.; Coppens, P.; Landrum, J. *Inorg. Chem.* **1988**, *27*, 482−488.
(22) Kachalova, G. S.; Popov, A. N.; Bartunik, H. D. *Science* **1999**, *284*, 475−476.
(23) Safo, M. K.; Gupta, G. P.; Walker, F. A.; Scheidt, W. R. *J. Am. Chem. Soc.* **1991**, *113*, 5497−5510.
(24) Ellison, M. K.; Scheidt, W. R. *J. Am. Chem. Soc.* **1997**, *119*, 7404−7405.
(25) Collman, J. P.; Hoard, J. L.; Kim, N.; Lang, G.; Reed, C. A. *J. Am. Chem. Soc.* **1975**, *97*, 2676−2681.
(26) Al-Abdalla, A.; Seijo, L.; Barandiarán, Z. *J. Chem. Phys.* **1998**, *109*, 6396−6405.

were taken from ref 11. In the case of the inorganic salts and the oxide $BaFeO_4$, small clusters were employed in the calculations,[2−4,15] i.e., $[Fe(CN)_6]^{4-}$ for $K_4[Fe(CN)_6]$, $[Fe(CN)_6]^{3-}$ for $K_3[Fe(CN)_6]$, $[FeF_6]^{4-}$ for $KFeF_3$, $[FeF_6]^{3-}$ for FeF_3, and $[FeO_4]^{2-}$ for $BaFeO_4$. For metalloporphyrins/metalloproteins, porphyrin substituents (such as phenyls) were replaced by hydrogens in exactly the same manner as reported previously for ^{57}Fe NMR chemical shift calculations.[9] The experimental isomer shift data[1,9,11,23,25,32−35] were all from the literature. For the basis set dependence studies on the inorganic complexes, we used STO-3G, 3-21G, 6-311G, and "locally dense" [36] split valence basis sets, the latter consisting of a Wachters' all electron basis for Fe (62111111/3311111/3111)[37] together with a 6-311G* basis for the other heavy atoms. For the metalloporphyrins, we used the Wachters' basis for Fe, 6-311G* for all heavy atoms, and 6-31G* for hydrogens. Numerous pure and hybrid exchange-correlation functionals were investigated in initial work, but only B3LYP and BPW91 functional results are discussed in the text (where B3LYP represents Becke's three-parameter functional[38] with the Lee, Yang, and Parr correlation functional[39] and BPW91 represents a pure DFT approach: Becke's 88 exchange[40] and a Perdew−Wang 91 correlation functional[41]), basically as described previously.[6,9] Results for other hybrid functionals described previously[9] did not give improved results. For diamagnetic systems restricted methods were used, while for paramagnetic systems spin-unrestricted methods were employed, i.e., UBPW91 and UB3LYP. To determine $\rho^{tot}(0)$ values and the different MO contributions to $\rho^{tot}(0)$, we used the AIM 2000 program.[19] Molecular orbitals were computed using Gaussian 98 and displayed using Cerius^2.[42]

Results and Discussion

Inorganic Systems and the Evaluation of α^{rel}. Molecular orbital calculations give information on the charge or electron density at the nucleus, $\rho^{tot}(0)$, which is related to the isomer shift via eq 2. However, the charge densities obtained via HF or DFT methods are, of course, not the fully relativistic values which might be obtained from Dirac−Fock theory. Consequently, it is customary to correct the nonrelativistic charge densities by use of a relativistic scaling factor S, and in most cases S is taken to be 1.30.[2,16] However, the evaluation of S has clearly been shown to be basis set dependent.[16] Moreover, it also seems possible that S may vary with the type of theory used to evaluate it. For example, HF methods ignore electron correlation effects, and as shown previously, HF methods do not permit the evaluation of ^{57}Fe (or ^{95}Mo or ^{103}Rh) metal ion NMR chemical shifts.[7,8] It is also possible that S values will depend on a given Fe d^n electron configuration and might also vary between the different s shells of the iron atom.[2] Clearly, then, it might simply be impossible to accurately evaluate ^{57}Fe Mössbauer isomer shifts in metalloporphyrins and related systems, since fully relativistic calculations on such large molecules are not currently feasible.

Table 1. Charge Densities at Iron for Different Calculational Methods and Basis Sets: Comparison with Relativistic Results

basis		$\Delta\rho^{rel}(0)$ (au)[a]	$\Delta\rho^{tot}(0)$ (au)[b]		
			HF	BPW91	B3LYP
6-311G	$3d^54s^1$	11.61	11.71	12.47	12.22
	$3d^64s^2$	9.35	8.97	9.56	10.60
	$3d^64s^1$	6.11	6.54	7.48	7.24
	$3d^54s^0$	3.01	3.04	2.89	2.89
Wachters'	$3d^54s^1$	11.61	11.57	12.31	12.05
	$3d^64s^2$	9.35	9.43	6.60[c]	9.74
	$3d^64s^1$	6.11	6.72	7.74	7.49
	$3d^54s^0$	3.01	2.89	2.70	2.70

[a] Relativistic charge densities, $\rho^{rel}(0)$, are from ref 3. $\Delta\rho^{rel}(0)$ is referenced to $\rho^{rel}(0)$ for the $3d^64s^0$ configuration. [b] $\Delta\rho^{tot}(0)$ is referenced to $\rho^{tot}(0)$ of $3d^64s^0$ and multiplied by the relativistic correction factor, S = 1.30. [c] The computed electronic state is $3d^{6.67}4s^{1.33}$, so its $\rho^{tot}(0)$ is smaller than expected for $3d^64s^2$.

To begin with, we first investigated the effects of calculational method (HF, DFT, hybrid HF-DFT; basis set dependence) on the prediction of the relativistic correction factors and thereby on $\rho^{tot}(0)$ for five different iron configurations, comparing these results with earlier relativistic results. The HF results were essentially identical to those of Yamada and Tominaga,[16] with minimal (STO-3G) and small (3-21G) basis sets giving apparent S values of 1.93 and 1.70, respectively, in poor accord with accepted values. However, the larger 6-311G and Wachters' basis sets yielded S = 1.30, independent of the calculational methods used, again in good accord with previous work.[2,16] We therefore used this value to deduce relativistically corrected charge densities in Table 1, where the computed $\Delta\rho^{tot}(0)$ values are given relative to those found for the $3d^64s^0$ configuration for HF, pure, and hybrid DFT methods using both 6-311G and Wachters' basis sets. It can be seen that there is generally good accord with the relativistic results, $\Delta\rho^{rel}(0)$.

Next, we investigated a α^{rel} prediction in a series of four inorganic systems, $K_4[Fe(CN)_6]$ ($S = 0$), $K_3[Fe(CN)_6]$ ($S = {}^1/_2$), $KFeF_3$ ($S = 2$), and FeF_3 ($S = {}^5/_2$), relatively small systems which cover all of the spin states commonly seen in metalloproteins and metalloporphyrins. These compounds have been investigated previously by Nieuwpoort et al.[4] using Hartree−Fock based methods and form a "benchmark" series with which to test the effects of using different DFT methods, as well as basis sets, on determination of the coefficient α^{rel}. Table 2 shows the $\rho^{tot}(0)$ values obtained on these four systems when using HF and DFT (BPW91, B3LYP) methods, as a function of basis set size. For the HF calculations, the small basis calculations give either poor correlations between $\rho^{tot}(0)$ and experiment or unusual α^{rel} values. However, for either the 6-311G or Wachter's Fe basis HF calculations, the R^2 values are quite high, and $\alpha^{rel} = -0.266\ a_0^3$ mm s^{-1} (6-311G) or $\alpha^{rel} = -0.253\ a_0^3$ mm s^{-1} (Wachters'). The rms error values are, however, also moderately high (0.25, 0.19 mm s^{-1} for 6-311G, Wachters', respectively). For the DFT calculations using the pure exchange-correlation

(27) Scheidt, W. R.; Geiger, D. K.; Lee, Y. J.; Reed, C. A.; Lang, G. *Inorg. Chem.* **1987**, *26*, 1039−1045.
(28) Vojtechovsky, J.; Berendzen, J.; Chu, K.; Schlichting, I.; Sweet, R. M. *Biophys. J.* **1999**, *77*, 2153−2174.
(29) Wilson, J.; Phillips, K.; Luisi, B. *J. Mol. Biol.* **1996**, *264*, 743−756.
(30) Scheidt, W. R.; Finnegan, M. G. *Acta Crystallogr.* **1989**, *C45*, 1214−1216.
(31) Skelton, B. W.; White, A. H. *Aust. J. Chem.* **1977**, *30*, 2655−2660.
(32) Kerler, W.; Neuwirth, W.; Fluck, E. *Z. Phys.* **1963**, *175*, 200.
(33) Kobayashi, H.; Maeda, Y.; Yanagawa, Y. *Bull. Chem. Soc. Jpn.* **1970**, *43*, 2342−2346.
(34) Bohle, D. S.; Debrunner, P.; Fitzgerald, J. P.; Hansert, B.; Hung, C.-H.; Thomson, A. J. *Chem. Commun.* **1997**, 91−92.
(35) Perkins, H. K.; Hazony, Y. *Phys. Rev. B* **1972**, *5*, 7−18.
(36) Chestnut, D. B.; Moore, K. D. *J. Comput. Chem.* **1989**, *10*, 648−659.
(37) Wachters, A. J. H. *J. Chem. Phys.* **1970**, *52*, 1033−1036. Wachters, A. J. H. IBM Technology Report RJ584, 1969. Basis sets were obtained from the Extensible Computational Chemistry Environment Basis Set Database, Version 1.0, as developed and distributed by the Molecular Science Computing Facility, Environmental and Molecular Science Laboratory, which is part of the Pacific Northwest Laboratory, P.O. Box 999, Richland, WA 99352, and is funded by the U.S. Department of Energy. The Pacific Northwest Laboratory is a multiprogram laboratory operated by Battelle Memorial Institute for the U.S. Department of Energy under contract DE-AC06-76RLO 1830. Contact David Feller, Karen Schuchardt, or Don Jones for further information.
(38) Becke, A. D. *J. Chem. Phys.* **1993**, *98*, 5648−52.
(39) Lee, C.; Yang, W.; Parr, R. G. *Phys. Rev. B* **1988**, *37*, 785−789.
(40) Becke, A. D. *Phys. Rev. A* **1988**, *38*, 3098−3100.
(41) Perdew, J. P.; Burke, K.; Wang, Y. *Phys. Rev. B* **1996**, *54*, 16533−16539.
(42) *Cerius^2 Modelling Environment*, Version 4.5; Molecular Simulation Inc., San Diego, CA, 2000.

Table 2. Effects of Basis Sets and Calculational Method on Computed Total Charge Densities at Iron

method	compounds	S	δ_{Fe}^{expt} (mm/s)[a]	$\rho^{tot}(0)$ (au) STO-3G	3-21G	6-311G	LDBS[b]
HF	$K_4[Fe(CN)_6]$	0	−0.07	7810.22	8879.61	11620.75	11623.53
	$K_3[Fe(CN)_6]$	$^1/_2$	−0.15	7810.42	8880.84	11622.01	11624.68
	$KFeF_3$	2	1.44	7808.95	8877.30	11616.77	11619.31
	FeF_3	$^5/_2$	0.69	7809.86	8880.49	11619.84	11622.26
	R^2			0.958	0.622	0.931	0.956
	α (relativistic)			−0.606	−0.351	−0.266	−0.253
	rms error (mm/s)			0.19	0.71	0.25	0.19
BPW91	$K_4[Fe(CN)_6]$	0	−0.07	7810.28	8876.30	11621.76	11617.45
	$K_3[Fe(CN)_6]$	$^1/_2$	−0.15	7810.29	8876.61	11622.10	11617.79
	$KFeF_3$	2	1.44	7811.57	8875.57	11618.85	11614.42
	FeF_3	$^5/_2$	0.69	7809.88	8875.77	11620.14	11615.75
	R^2			0.490	0.895	0.993	0.993
	α (relativistic)			0.750	−0.971	−0.381	−0.367
	rms error (mm/s)			0.93	0.31	0.07	0.07
B3LYP	$K_4[Fe(CN)_6]$	0	−0.07	7810.26	8876.56	11617.14	11614.15
	$K_3[Fe(CN)_6]$	$^1/_2$	−0.15	7810.27	8876.95	11617.56	11614.57
	$KFeF_3$	2	1.44	7811.56	8876.27	11613.60	11610.55
	FeF_3	$^5/_2$	0.69	7809.87	8876.39	11615.74	11612.60
	R^2			0.497	0.714	0.989	0.994
	α (relativistic)			0.742	−1.75	−0.323	−0.316
	rms error (mm/s)			0.92	0.58	0.10	0.07

[a] Experimental δ_{Fe} values are from low-temperature experiments or extrapolated to low temperature, as shown in Table 3. [b] This designates the locally dense basis set described in the Experimental Section.

functional (BPW91), the R^2 values are clearly higher than those obtained by using HF theory and the rms error values are also very good (0.07 mm s^{-1}), but the α values for the larger basis calculations are also higher ($\alpha^{rel} = -0.381$, -0.367 a_0^3 mm s^{-1}). Finally, for the hybrid DFT (B3LYP) method (which contains 20% HF exchange), the R^2 values for the two larger basis calculations are again very good (0.989, 0.994), the rms error values are good (0.10, 0.07 mm s^{-1}), and in addition, the α^{rel} values decrease to -0.323, -0.316 a_0^3 mm s^{-1}. As can be seen in Table 2, there is convergence in the basis at about the 6-311G level for α^{rel} values as a function of basis set size, for HF, B3LYP, and BPW91 DFT calculations. For the HF calculation, we find $\alpha^{rel} = -0.253$ a_0^3 mm s^{-1}, essentially the -0.22 ± 0.02 a_0^3 mm s^{-1} value reported previously by others[4] and in very good accord with the "consensus" value of -0.267 ± 0.115 a_0^3 mm s^{-1}, but for the pure density functional BPW91, $\alpha^{rel} = -0.381$ to -0.367 a_0^3 mm s^{-1}. This is clearly larger than the consensus value of α but still within the range of -0.267 ± 0.115 a_0^3 mm s^{-1} reported over the years, and the rms error and R^2 values are also clearly improved over the HF calculation. These initial results clearly indicate, therefore, that better R^2 and rms error results are obtained by using the DFT method. However, the values of α^{rel} obtained appear to be too high when using the pure density functional. On the other hand, HF methods ignore electron correlation and do not permit accurate evaluation of other properties such as metal ion (e.g., ^{57}Fe) NMR chemical shifts, so one must question the quality of pure HF wave functions. We therefore next investigated the use of the hybrid B3LYP functional. As noted above, the B3LYP functional incorporates the effects of both electron correlation and HF exchange and has been found to permit the accurate prediction of both local (^{57}Fe NMR chemical shifts, chemical shift anisotropies, ^{57}Fe Mössbauer quadrupole splittings) and nonlocal (^2H, ^{13}C, ^{15}N, ^{19}F NMR hyperfine shift) spectroscopic properties. As shown in Table 2, by using the large Wachters' basis, we obtain excellent R^2 and rmsd values (0.994, 0.07 mm s^{-1}) in addition to a much smaller α^{rel} of -0.316 a_0^3 mm s^{-1}. This value is only 18% higher than the "consensus" value of -0.267 ± 0.115 a_0^3 mm s^{-1} and is well within one standard deviation of the accepted value. These results suggest, therefore, that at least part of the origin of the variations in α arises from neglect of electron correlation in HF (or other, semiempirical) calculations. Since we also know that HF methods do not permit ^{57}Fe NMR shift calculations, while DFT methods do permit such calculations—as well as ^{57}Fe Mössbauer quadrupole splittings[9]—it appeared that DFT methods might also be more appropriate for $\delta_{Fe}/\rho^{tot}(0)$, isomer shift/charge density calculations, in both inorganic and organometallic systems. We therefore next tested this hypothesis by investigating δ_{Fe} predictions in 20 different systems (24 structures) covering all spin states and a very wide range of δ_{Fe} values.

Since both of the DFT methods gave excellent R^2 and rmsd results for the four small inorganic systems (Table 2), we evaluated $\delta_{Fe}/\rho^{tot}(0)$ values with both the pure DFT (BPW91) and hybrid (B3LYP) functionals to see to what extent the experimental results could be reproduced by the calculations. The molecules or systems chosen cover the range of isomer shifts from -0.90 to 1.44 mm s^{-1}, all spin states, and Fe(0), Fe(II), Fe(III), and Fe(VI) oxidation states and include numerous metalloporphyrins and metalloproteins. These calculations cover, therefore, most of the major types of Fe bonding seen experimentally. They also provide a test of a number of potential problems with predicting δ_{Fe}: Are protein crystal structures sufficiently accurate to enable δ_{Fe} predictions? Does the neglect of second-order Doppler effects prevent accurate δ_{Fe} calculations in the systems investigated? Are the δ_{Fe} predictions accurate? Are the α values reasonable? Are there particular problems associated with any specific spin state or oxidation state? Are there problems associated with the use of Gaussian type basis functions? Do numerical basis sets have to be employed? Are there any indications of the need for fully relativistic calculations?

As shown in Figure 1A and Table 3, we first found an excellent correlation between δ_{Fe} and $\rho^{tot}(0)$ for the BPW91

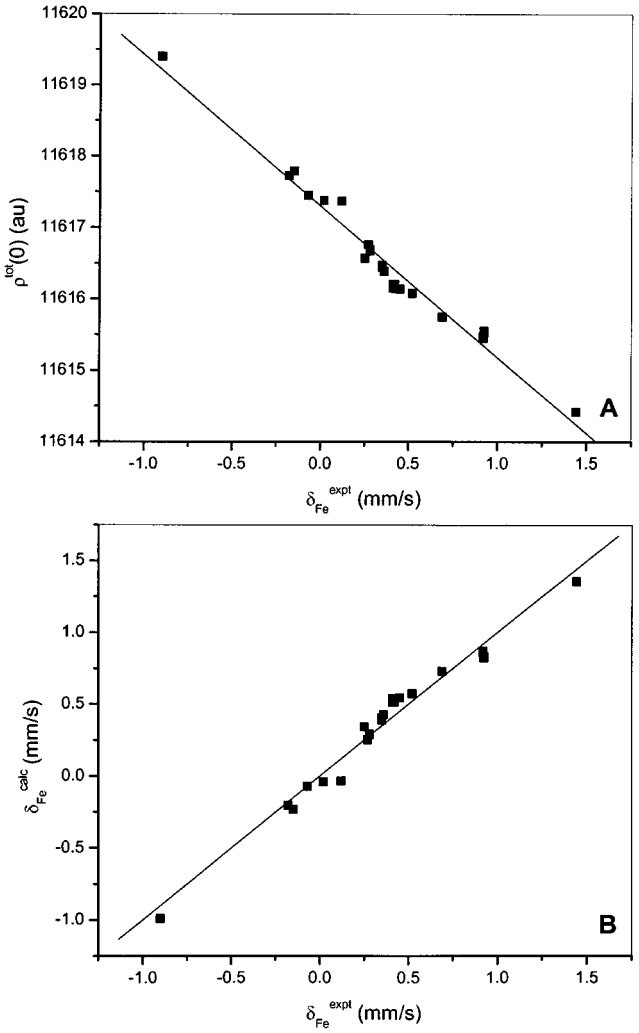

Figure 1. Graphs showing correlation between experimental ^{57}Fe Mössbauer isomer shifts (δ_{Fe}) and (A) the total charge density at the ^{57}Fe nucleus, $\rho^{tot}(0)$, computed by using the BPW91 functional and the Wachters' Fe basis and (B) δ_{Fe} computed from eq 4.

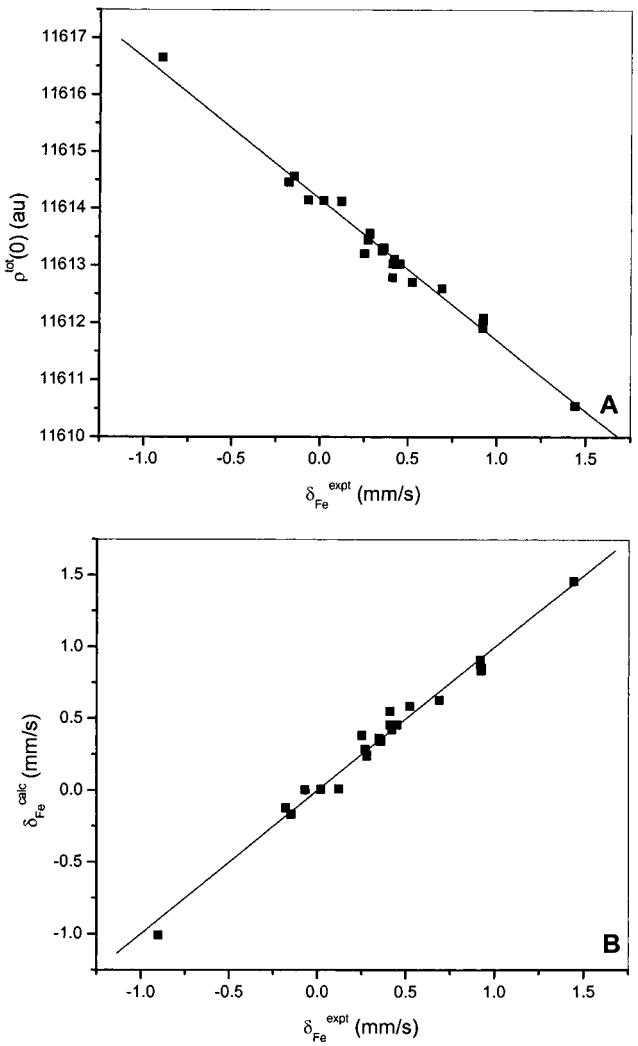

Figure 2. Graphs showing correlation between experimental ^{57}Fe Mössbauer isomer shifts (δ_{Fe}) and (A) the total charge density at the ^{57}Fe nucleus, $\rho^{tot}(0)$, computed by using the B3LYP functional and Wachters' Fe basis and (B) δ_{Fe} computed from eq 6.

correlation, and the results shown can be expressed by the following equation:

$$\rho^{tot}(0) = -2.123\delta_{Fe} + 11617.30 \quad (3)$$

or alternatively, the ^{57}Fe Mössbauer isomer shift is given by

$$\delta_{Fe} = -0.471[\rho^{tot}(0) - 11617.30] \quad (4)$$

For the 20 compounds investigated (24 computed structures, Table 3), we find $R^2 = 0.973$, $\alpha = -0.471$ a_0^3 mm s^{-1}, corresponding to a relativistically corrected $\alpha^{rel} = -0.362$ a_0^3 mm s^{-1}, using the S = 1.30 value computed previously. When these δ_{Fe} values are plotted versus experiment (Figure 1B), we find an rms error of 0.080 mm s^{-1} for the 2.34 mm s^{-1} range. The relativistically corrected value of $\alpha^{rel} = -0.362$, is, however, arguably too high, as might also be expected on the basis of the four model compound results (Table 2), although it could perhaps also be argued that any HF or semiempirically derived α values are too low, due to the complete neglect of electron correlation. In any case, we next computed the $\rho^{tot}(0)$ values using the B3LYP hybrid XC functional (which contains the effects of both electron correlation and HF exchange) and obtained the results shown in Table 3 and Figure 2. Figure 2A shows the correlation between δ_{Fe} and $\rho^{tot}(0)$ and can be fitted by

$$\rho^{tot}(0) = -2.475\delta_{Fe} + 11614.16 \quad (5)$$

or alternatively, the ^{57}Fe Mössbauer isomer shift is given by

$$\delta_{Fe} = -0.404[\rho^{tot}(0) - 11614.16] \quad (6)$$

For the 20 compounds investigated (24 calculated points), we find $R^2 = 0.981$ and a relativistically corrected $\alpha^{rel} = -0.311$ a_0^3 mm s^{-1} (using S = 1.30). Figure 2B shows the calculation versus experiment δ_{Fe} correlation, where there is a 0.067 mm s^{-1} rms error, corresponding to only 2.86% of the entire 2.34 mm s^{-1} range of δ_{Fe} values. Thus, the B3LYP calculations provide both a better R^2 value (0.981 versus 0.973) and a more conventional, relativistically corrected $\alpha^{rel} = -0.311$ a_0^3 mm s^{-1} value, consistent, we believe, with the better performance of B3LYP in computing the ^{57}Fe NMR and other spectroscopic observables reported previously.[8,9] These results are of considerable interest, since they clearly show that it is now possible to evaluate δ_{Fe} for all six Fe spin states: the R^2 value is as high

Table 3. Experimental ^{57}Fe Mössbauer Isomer Shifts, Computed Charge Densities at Iron, and Computed Isomer Shifts for Metalloporphyrins/Metalloproteins and Model Systems

	compound	structure[a]	S	δ_{Fe}^{expt} [b] (mm/s)	T (K)	$\rho^{tot}(0)$ (au) BPW91	$\rho^{tot}(0)$ (au) B3LYP	δ_{Fe}^{calc} [c] (mm/s) BPW91	δ_{Fe}^{calc} [c] (mm/s) B3LYP
1	$K_4[Fe^{II}(CN)_6]$	[4]	0	−0.07[32]	143	11617.45	11614.15	−0.07	0.00
2	$Fe(CO)_5$	[11]	0	−0.18[32]	143	11617.73	11614.46	−0.20	−0.12
3	$Fe(CO)_3$(cyclobutadiene)	[11]	0	0.02[11]	77	11617.38	11614.14	−0.04	0.01
4	$Fe(CO)_3$(1,4-dibutadiene)	[11]	0	0.12[11]	4.2	11617.37	11614.13	−0.03	0.01
5	Fe(TPP)(1-MeIm)(*i*-PrNC)	[20]	0	0.25[9]	77	11616.57	11613.21	0.34	0.38
6	$Fe(TPP)(pyr)_2$	[21]	0	0.41[33]	77	11616.21	11612.79	0.51	0.55
7	carbonmonoxymyoglobin	[22]	0	0.27[1]	4.2	11616.76	11613.45	0.25	0.29
	$[Fe(TMP)(N\text{-}MeIm)_2]ClO_4$[d]		$^1/_2$	0.28[23]	4.2				
8	molecule 1	[23]				11616.69	11613.57	0.29	0.24
9	molecule 2	[23]				11616.67	11613.55	0.30	0.25
	Fe(OEP)(NO)[e]		$^1/_2$	0.35[34]	100				
10	Fe(OEP)(NO)	[24]				11616.44	11613.26	0.41	0.36
11	Fe(OEP)(NO)	[24]				11616.47	11613.30	0.39	0.35
12	$K_3[Fe^{III}(CN)_6]$	[4]	$^1/_2$	−0.15[32]	143	11617.79	11614.57	−0.23	−0.17
13	Fe(TPP)	[25]	1	0.52[25]	4.2	11616.08	11612.71	0.57	0.59
14	$Fe^{VI}O_4^{2-}$	[26]	1	−0.90[32]	143	11619.40	11616.65	−0.99	−1.01
15	$[Fe(OEP)(3\text{-}Clpy)]ClO_4$	[27]	$^3/_2$	0.36[1]	4.2	11616.39	11613.31	0.43	0.34
	deoxymyoglobin[f]		2	0.92[1]	4.2				
16	1BZP	[22]				11615.45	11611.99	0.87	0.88
17	1A6N	[28]				11615.47	11611.91	0.86	0.91
	deoxyhemoglobin[g]		2	0.92_5[1]	4.2				
18	α-chain	[29]				11615.55	11612.09	0.82	0.84
19	β-chain	[29]				11615.53	11612.04	0.83	0.86
20	$KFe^{II}F_3$	[4]	2	1.44[35]	0	11614.42	11610.55	1.36	1.46
21	Fe(TPP)Cl	[30]	$^5/_2$	0.41[1]	4.2	11616.15	11613.03	0.54	0.46
22	metmyoglobin	[22]	$^5/_2$	0.42[1]	4.2	11616.21	11613.11	0.51	0.42
23	Fe(TPP)Br	[31]	$^5/_2$	0.45[1]	4.2	11616.14	11613.03	0.55	0.46
24	$Fe^{III}F_3$	[4]	$^5/_2$	0.69[35]	0	11615.75	11612.60	0.73	0.63

[a] References for structures are provided in brackets. [b] The experimental references for isomer shifts are listed as superscripts. [c] Computed by using eqs 4 and 6, respectively, for BPW91 and B3LYP. [d] Two molecules in the unit cell. [e] Two different crystal structures for the same molecule, Cambridge Structural Database IDs RIQSUF and RIQSUF01 for **10** and **11**, respectively. [f] PDB structure codes for **16**, **17** shown below. [g] Two subunits from the same PDB file 1IBE.

Table 4. Effects of Coordinate Precision on Computed $\rho^{tot}(0)$ Values (au)

method	deoxyhemoglobin	$n=3$	$n=4$	$n=5$	$n=6$	$n=7$	$n=8$
BPW91	α-chain	11556.23	11615.10	11615.54	11615.55	11615.55	11615.55
	β-chain	11576.08	11614.06	11615.52	11615.53	11615.53	11615.53
	difference	19.85	1.04	0.02	0.02	0.02	0.02
B3LYP	α-chain	11552.79	11611.64	11612.08	11612.09	11612.09	11612.09
	β-chain	11572.61	11610.57	11612.03	11612.04	11612.04	11612.04
	difference	19.82	1.07	0.05	0.05	0.05	0.05

as 0.981, the rms error as low as 0.067 mm s^{-1}, and $\alpha^{rel} = -0.311\ a_0^3$ mm s^{-1}. The statistical probability that the R^2 value is zero is $p < 0.0001$.

The observation of such large R^2 values and small rms errors strongly suggests that the use of the large, locally dense basis set approach should be generally applicable to other inorganic as well as organometallic/metalloporphyrin/metalloprotein systems, independent of oxidation or spin state. For example, even the previously difficult system $[FeO_4]^{2-}$ ($S = 1$),[3] which has an experimental $\delta_{Fe} = -0.90$ mm s^{-1}, is quite well reproduced in the present calculations (−0.99, −1.01 mm s^{-1}, BPW91, B3LYP). While it might be argued that such good overall agreement between calculation and experiment is simply fortuitous and that fully relativistic, second-order Doppler corrected calculations need to be employed, possibly using crystallographic structures determined at 4.2 K, and that all δ_{Fe} values should be determined at 4.2 K (or lower), the $p < 0.0001$ value ($N = 24$), rms error (0.067 mm s^{-1}; 2.34 mm s^{-1} range), and $\alpha^{rel} = -0.311\ a_0^3$ mm s^{-1} values would seem to argue against this. Indeed, the uniform $S = 1.30$ value has been used in many previous studies,[2,15−17] and in 15 of the systems investigated, δ_{Fe} results are already reported at very low temperatures, where second-order Doppler effects are expected to be negligible, and the results obtained on these systems are not statistically different from those obtained at the higher temperatures.

What, then, are the major contributions to the small residual errors seen between calculation and experiment? In some early calculations, we found in the α and β subunits of deoxyhemoglobin that there were quite large differences between $\rho(0)$ for the two iron sites, which are simply not reflected in the experimental values of δ_{Fe}. While we initially thought that this might just be due to crystallographic uncertainties (because deoxyhemoglobin is a very large molecule), on further investigation we found that this was not the case. Rather, we found that truncating the precision of the Cartesian coordinates in the wave function files ($n = 8$ decimal places) generated by Gaussian 98 when being read into the AIM2000 program could result in erroneous charge densities. Computed $\rho^{tot}(0)$ results for the α and β chains for $n = 3-8$ are given in Table 4. Clearly, for $n = 4$, there are 1.04 (BPW91) and 1.07 au (B3LYP) differences in $\rho(0)$ between the two chains, but this decreases

to 0.02 (BPW91), 0.05 au (B3LYP) at $n = 5$, and $\rho^{tot}(0)$ is essentially constant for $n \geq 6$. For the B3LYP calculations, the computed δ_{Fe} values are 0.84 and 0.86 mm s^{-1} for the α and β subunits, close to the 0.92_5 reported experimentally.[1] For deoxymyoglobin, we obtain $\delta_{Fe} = 0.88$ and 0.91 mm s^{-1} for the 1BZP and 1A6N structures, respectively, in even better accord with the experimental value of 0.92 mm s^{-1}. This improvement may be related to the higher resolution (1.15 Å) of the myoglobin structure over the 1.80 Å resolution of the 1IBE structure used for the deoxyhemoglobin α and β chain calculations.

These theoretical results appear encouraging in that they enable the accurate prediction of δ_{Fe} values for a wide range of compounds using calculational methods which have been thoroughly tested by several groups in the calculation of other spectroscopic properties, such as NMR chemical shifts and NMR hyperfine shifts. This leads to the conclusion that the wave functions so obtained are quite reliable and that there might be additional information of interest in the actual magnitudes of the various contributions to $\rho^{tot}(0)$, the charge density at the nucleus. In the results discussed above, we just looked at $\rho^{tot}(0)$, the total charge density at the nucleus. However, using the AIM2000 program,[19] it is possible to obtain the various MO contributions to $\rho(0)$. This basic approach has been investigated previously by other workers.[2−4] However, with other than minimal basis sets (which do not permit accurate prediction of the other spectroscopic observables), it is not possible to break down the MO contributions into pure Fe 1s, 2s etc. atomic orbital contributions, but it is possible to investigate the individual MOs, which may be of primarily Fe 1s, 2s etc. character, basically as described below. To begin with, we therefore investigated the four inorganic systems described above: $K_4[Fe^{II}(CN)_6]$ ($S = 0$), $K_3[Fe^{III}(CN)_6]$ ($S = {}^1/_2$), $KFe^{II}F_3$ ($S = 2$), and $Fe^{III}F_3$ ($S = {}^5/_2$). Again, we used HF, pure DFT (BPW91), and hybrid HF-DFT (B3LYP) methods with four different basis sets. In all calculations, we found that there were three single "core" MOs (for each spin up and spin down state) making the major contribution to the total charge density, as noted previously by Nieuwpoort et al.[4] The variations in the computed $\rho^{tot}(0)$ values with chemical structure were very small for the three core MOs, as evidenced, for example, by the rmsd values shown in Table 5. However, the "valence" MO contributions (summed over all upper occupied MOs, not pure AOs), $\rho_{val}(0)$, although they make the smallest overall contribution to $\rho^{tot}(0)$, were found to vary considerably between the different chemical structures. The results of Table 5 are also of interest in that they show that the individual $\rho(0)$ contributions vary somewhat with basis set size and method of calculation. However, as the basis set size increases, and on introduction of electron correlation (in the DFT calculations), an arguably more chemically reasonable picture arises in which both the variance and even more clearly the overall *range* in $\rho(0)$ values follow the pattern, $\Delta|\rho_{val}(0)| \gg \Delta|\rho_i(0)|$ ($i = 1$, 2, and 3, where $\rho_i(0)$ is charge density contribution from the ith core MO). This effect was also noted in early work by Walker, Simanek, and others.[15a,h,43] That is, the core MOs (primarily Fe 1s, 2s, 3s atomic orbitals), which contribute ~99.9% to $\rho^{tot}(0)$, are essentially invariant to changes in the chemistry, while the higher occupied MO contributions ($\rho_{val}(0)$) are extremely sensitive to changesin chemical bonding, even though they contribute only ~0.1% to $\rho^{tot}(0)$.

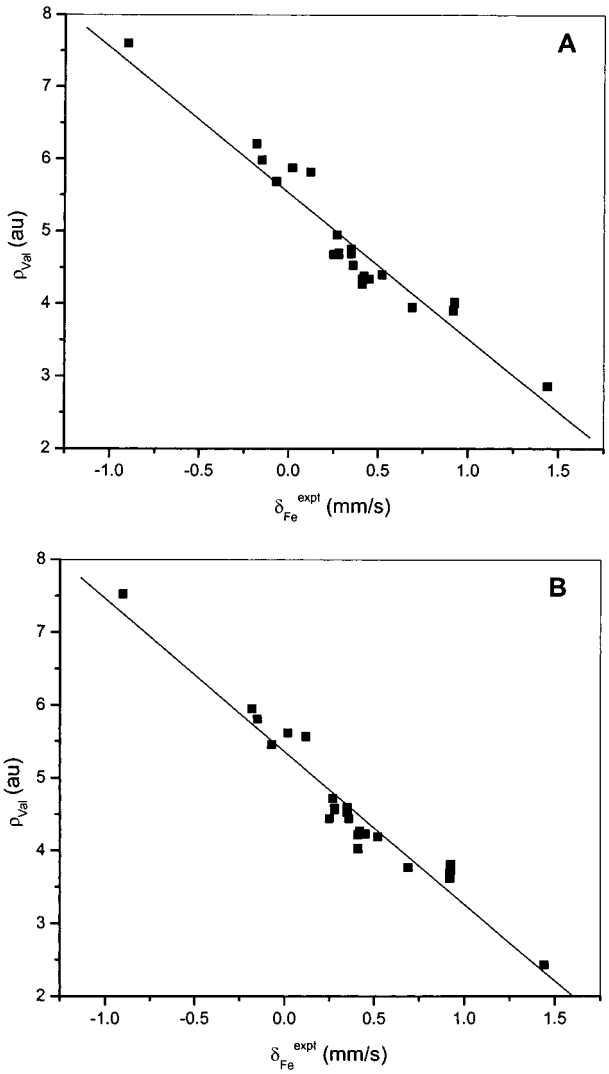

Figure 3. Graphs showing correlations between δ_{Fe} (expt) and the sum of the valence $\rho(0)$ contributions to the total charge density. **(**A) BPW91 calculations and (B) B3LYP calculations. Data from Tables 6 and 7.

To investigate this effect in more detail, we then computed the MO contributions to $\rho(0)$ for all of the 24 structures shown in Table 3, covering the full 2.34 mm s^{-1} range: $S = 0$, $^1/_2$, 1, $^3/_2$, 2, and $^5/_2$ as well as d^2, d^5, d^6, and d^8 iron configurations. We show in Tables 6 and 7 the various contributions to $\rho^{tot}(0)$ from the BPW91 and B3LYP calculations. These results show that there is very little variation in the core MO $\rho(0)$ values for a given calculational method, and in fact essentially all of the variation in $\rho^{tot}(0)$ is given in the $\rho_{val}(0)$ contributions, which are, however, those which might reasonably be expected to reflect the changes in chemical bonding that exist between the different chemical systems. This result is not at variance with previous conclusions from valence-electron-only calculations, where the dominant change in $\rho^{tot}(0)$ arises from the $\rho_{3s}(0)$ contribution.[5] In those calculations, the core contributions are orthogonalized to the valence MOs in order to account for polarization effects, whereas in our approach the admixture of the core atomic orbitals to the valence molecular orbitals, and

(43) Watson, R. E. Technical Report No. 12, Solid State and Molecular Theory Group, Massachusetts Institute of Technology, 1959 (unpublished).

Table 5. Effects of Computational Method and Basis Sets on Different MO Contributions to the Total Charge Densities at Iron

method	basis set	compound	S	$\rho_1(0)$	$\rho_2(0)$	$\rho_3(0)$	$\rho_{val}(0)$
HF	STO-3G	$K_4[Fe^{II}(CN)_6]$	0	6773.65	921.49	111.88	3.20
		$K_3[Fe^{III}(CN)_6]$	$^1/_2$	6773.64	921.70	111.96	3.12
		$KFe^{II}F_3$	2	6773.73	921.39	112.02	1.81
		$Fe^{III}F_3$	$^5/_2$	6773.68	922.04	112.16	1.98
		rmsd		0.04	0.29	0.12	0.73
	3-21G	$K_4[Fe^{II}(CN)_6]$	0	8026.60	741.41	107.95	3.65
		$K_3[Fe^{III}(CN)_6]$	$^1/_2$	8026.58	741.46	108.79	4.01
		$KFe^{II}F_3$	2	8027.87	740.74	107.42	1.27
		$Fe^{III}F_3$	$^5/_2$	8027.78	740.89	109.48	2.34
		rmsd		0.71	0.36	0.91	1.26
	6-311G	$K_4[Fe^{II}(CN)_6]$	0	10456.16	1018.76	141.28	4.55
		$K_3[Fe^{III}(CN)_6]$	$^1/_2$	10455.99	1018.72	142.24	1.06
		$KFe^{II}F_3$	2	10456.65	1018.61	139.89	1.62
		$Fe^{III}F_3$	$^5/_2$	10456.25	1018.47	142.14	2.98
		rmsd		0.28	0.13	1.09	1.56
	LDBS[a]	$K_4[Fe^{II}(CN)_6]$	0	10456.79	1020.62	141.41	4.71
		$K_3[Fe^{III}(CN)_6]$	$^1/_2$	10456.63	1020.56	142.28	5.21
		$KFe^{II}F_3$	2	10457.29	1020.43	140.00	1.59
		$Fe^{III}F_3$	$^5/_2$	10456.88	1020.29	142.19	2.90
		rmsd		0.28	0.15	1.05	1.67
BPW91	STO-3G	$K_4[Fe^{II}(CN)_6]$	0	6772.45	918.48	115.84	3.51
		$K_3[Fe^{III}(CN)_6]$	$^1/_2$	6772.45	918.51	115.86	3.47
		$KFe^{II}F_3$	2	6772.48	918.77	115.99	4.33
		$Fe^{III}F_3$	$^5/_2$	6772.49	918.67	115.97	2.75
		rmsd		0.02	0.14	0.08	0.65
	3-21G	$K_4[Fe^{II}(CN)_6]$	0	8025.18	735.20	111.37	4.55
		$K_3[Fe^{III}(CN)_6]$	$^1/_2$	8025.18	735.19	111.50	4.74
		$KFe^{II}F_3$	2	8026.58	734.74	111.62	2.63
		$Fe^{III}F_3$	$^5/_2$	8026.51	734.69	111.47	3.10
		rmsd		0.79	0.28	0.10	1.05
	6-311G	$K_4[Fe^{II}(CN)_6]$	0	10461.32	1008.61	146.22	5.61
		$K_3[Fe^{III}(CN)_6]$	$^1/_2$	10461.28	1008.58	146.34	5.90
		$KFe^{II}F_3$	2	10461.69	1008.72	145.42	3.02
		$Fe^{III}F_3$	$^5/_2$	10461.53	1008.61	145.95	4.05
		rmsd		0.19	0.06	0.41	1.35
	LDBS[a]	$K_4[Fe^{II}(CN)_6]$	0	10454.93	1010.48	146.35	5.69
		$K_3[Fe^{III}(CN)_6]$	$^1/_2$	10454.89	1010.44	146.47	5.99
		$KFe^{II}F_3$	2	10455.30	1010.61	145.65	2.86
		$Fe^{III}F_3$	$^5/_2$	10455.13	1010.48	146.18	3.95
		rmsd		0.19	0.07	0.36	1.48
B3LYP	STO-3G	$K_4[Fe^{II}(CN)_6]$	0	6772.32	919.33	115.16	3.45
		$K_3[Fe^{III}(CN)_6]$	$^1/_2$	6772.32	919.37	115.18	3.40
		$KFe^{II}F_3$	2	6772.36	919.66	115.35	4.19
		$Fe^{III}F_3$	$^5/_2$	6772.37	919.56	115.34	2.60
		rmsd		0.03	0.16	0.10	0.65
	3-21G	$K_4[Fe^{II}(CN)_6]$	0	8025.01	736.46	110.75	4.34
		$K_3[Fe^{III}(CN)_6]$	$^1/_2$	8025.00	736.45	110.95	4.55
		$KFe^{II}F_3$	2	8026.38	735.97	111.37	2.55
		$Fe^{III}F_3$	$^5/_2$	8026.31	735.92	111.17	2.99
		rmsd		0.77	0.30	0.27	0.99
	6-311G	$K_4[Fe^{II}(CN)_6]$	0	10456.24	1010.08	145.46	5.36
		$K_3[Fe^{III}(CN)_6]$	$^1/_2$	10456.19	1010.04	145.64	5.69
		$KFe^{II}F_3$	2	10456.68	1010.12	144.24	2.56
		$Fe^{III}F_3$	$^5/_2$	10456.41	1009.96	145.48	3.89
		rmsd		0.22	0.07	0.65	1.44
	LDBS[a]	$K_4[Fe^{II}(CN)_6]$	0	10451.14	1011.96	145.59	5.46
		$K_3[Fe^{III}(CN)_6]$	$^1/_2$	10451.08	1011.90	145.77	5.81
		$KFe^{II}F_3$	2	10451.58	1012.02	144.49	2.43
		$Fe^{III}F_3$	$^5/_2$	10451.30	1011.85	145.67	3.77
		rmsd		0.22	0.07	0.60	1.57

[a] This designates the locally dense basis set described in the Experimental Section.

thus part of the core polarization, is assigned to the valence MO contribution.

This effect can be seen most clearly in Figure 3, where we plot the experimental δ_{Fe} values as a function of the computed $\rho_{val}(0)$. The statistics are, for BPW91, $R^2 = 0.915$, $N = 24$, $p < 0.0001$, and for B3LYP, $R^2 = 0.938$, $N = 24$, $p < 0.0001$. And, as expected, the correlation between the valence $\rho(0)$ and the total $\rho(0)$ (Figure 4) is also extremely high. For BPW91, $R^2 = 0.976$, $N = 24$, $p < 0.0001$, and for B3LYP, $R^2 = 0.965$, $N = 24$, $p < 0.0001$. These results strongly suggest, therefore, that it is the valence MO $\rho(0)$ which is primarily responsible for the changes in $\rho^{tot}(0)$, due to changes in chemical bonding, as opposed to the core MO $\rho(0)$ contributions, which are remarkably constant in all 24 systems. Also, these results do not give any evidence to support the idea that there are large changes in relativistic scaling factor S which depend on Fe d^n

Table 6. MO (α,β) Contributions to the Total Charge Densities at Iron (BPW91)[a]

	compound	S	$\rho_1^\alpha(0)$	$\rho_1^\beta(0)$	$\Delta\rho_1(0)$	$\rho_2^\alpha(0)$	$\rho_2^\beta(0)$	$\Delta\rho_2(0)$	$\rho_3^\alpha(0)$	$\rho_3^\beta(0)$	$\Delta\rho_3(0)$	$\rho_{val}^\alpha(0)$	$\rho_{val}^\beta(0)$	$\Delta\rho_{val}(0)$
1	$K_4[Fe^{II}(CN)_6]$	0	5227.46		−0.37	505.24		−0.13	73.17		0.70	2.85		2.83
2	$Fe(CO)_5$	0	5227.45		−0.41	505.22		−0.16	73.09		0.53	3.11		3.35
3	$Fe(CO)_3$(cyclobutadiene)	0	5227.47		−0.36	505.24		−0.13	73.04		0.43	2.94		3.02
4	$Fe(CO)_3$(1,4-dibutadiene)	0	5227.47		−0.35	505.24		−0.13	73.06		0.48	2.91		2.96
5	Fe(TPP)(1-MeIm)(*i*-PrNC)	0	5227.53		−0.23	505.28		−0.06	73.14		0.62	2.34		1.82
6	$Fe(TPP)(pyr)_2$	0	5227.55		−0.19	505.29		−0.03	73.12		0.6	2.14		1.41
7	carbonmonoxymyoglobin	0	5227.53		−0.25	505.27		−0.06	73.11		0.57	2.47		2.09
8	$[Fe(TMP)(N\text{-}MeIm)_2]ClO_4$	$^1/_2$	5227.52	5227.53	−0.25	505.06	505.47	−0.08	73.31	73.10	0.76	2.39	2.31	1.84
9	$[Fe(TMP)(N\text{-}MeIm)_2]ClO_4$	$^1/_2$	5227.52	5227.53	−0.25	505.06	505.47	−0.08	73.31	73.10	0.76	2.39	2.29	1.82
10	Fe(OEP)(NO)	$^1/_2$	5227.55	5227.55	−0.20	505.08	505.47	−0.05	73.15	72.94	0.44	2.44	2.25	1.83
11	Fe(OEP)(NO)	$^1/_2$	5227.54	5227.55	−0.21	505.08	505.47	−0.06	73.15	72.93	0.43	2.47	2.28	1.89
12	$K_3[Fe^{III}(CN)_6]$	$^1/_2$	5227.44	5227.45	−0.41	505.02	505.42	−0.17	73.33	73.13	0.82	3.05	2.95	3.13
13	Fe(TPP)	1	5227.58	5227.59	−0.13	504.87	505.72	−0.02	73.17	72.76	0.27	2.50	1.90	1.54
14	$Fe^{VI}O_4^{2-}$	1	5227.39	5227.40	−0.51	504.87	505.53	−0.20	73.52	73.09	0.95	3.83	3.77	4.74
15	$[Fe(OEP)(3\text{-}Clpy)]ClO_4$	$^3/_2$	5227.55	5227.56	−0.19	504.71	505.82	−0.07	73.40	72.81	0.56	2.47	2.06	1.67
16	deoxymyoglobin 1BZP	2	5227.60	5227.62	−0.08	504.53	506.04	−0.03	73.25	72.48	0.08	2.18	1.74	1.06
17	deoxymyoglobin 1A6N	2	5227.60	5227.62	−0.09	504.46	506.10	−0.05	73.32	72.47	0.15	2.14	1.76	1.04
18	deoxyhemoglobin α	2	5227.60	5227.61	−0.09	504.55	506.02	−0.04	73.26	72.49	0.10	2.23	1.79	1.16
19	deoxyhemoglobin β	2	5227.60	5227.62	−0.09	504.47	506.09	−0.05	73.30	72.46	0.11	2.24	1.76	1.14
20	$KFe^{II}F_3$	2	5227.64	5227.66	0.00	504.42	506.19	0.00	73.28	72.37	0.00	1.54	1.32	0.00
21	Fe(TPP)Cl	$^5/_2$	5227.55	5227.58	−0.17	504.36	506.16	−0.09	73.57	72.59	0.51	2.32	2.02	1.48
22	metmyoglobin	$^5/_2$	5227.55	5227.57	−0.18	504.31	506.18	−0.12	73.61	72.61	0.57	2.38	2.00	1.52
23	Fe(TPP)Br	$^5/_2$	5227.56	5227.58	−0.16	504.37	506.15	−0.09	73.55	72.59	0.49	2.33	2.01	1.48
24	$Fe^{III}F_3$	$^5/_2$	5227.55	5227.58	−0.17	504.24	506.25	−0.13	73.65	72.54	0.53	2.08	1.87	1.09
	rmsd				0.12			0.05			0.25			0.99

[a] $\Delta\rho_i(0)$ (i = 1, 2, 3, val) are referenced to the data of $KFe^{II}F_3$.

Table 7. MO (α,β) Contributions to the Total Charge Densities at Iron (B3LYP)[a]

	compound	S	$\rho_1^\alpha(0)$	$\rho_1^\beta(0)$	$\Delta\rho_1(0)$	$\rho_2^\alpha(0)$	$\rho_2^\beta(0)$	$\Delta\rho_2(0)$	$\rho_3^\alpha(0)$	$\rho_3^\beta(0)$	$\Delta\rho_3(0)$	$\rho_{val}^\alpha(0)$	$\rho_{val}^\beta(0)$	$\Delta\rho_{val}(0)$
1	$K_4[Fe^{II}(CN)_6]$	0	5225.57		−0.44	505.98		−0.06	72.79		1.10	2.73		3.03
2	$Fe(CO)_5$	0	5225.55		−0.49	505.97		−0.08	72.74		1.00	2.97		3.52
3	$Fe(CO)_3$(cyclobutadiene)	0	5225.57		−0.44	505.98		−0.06	72.70		0.91	2.81		3.19
4	$Fe(CO)_3$(1,4-dibutadiene)	0	5225.57		−0.43	505.98		−0.05	72.72		0.95	2.79		3.14
5	Fe(TPP)(1-MeIm)(*i*-PrNC)	0	5225.64		−0.3	506.01		0.00	72.73		0.98	2.22		2.01
6	$Fe(TPP)(pyr)_2$	0	5225.66		−0.25	506.02		0.02	72.70		0.90	2.02		1.60
7	carbonmonoxymyoglobin	0	5225.63		−0.32	506.01		−0.01	72.73		0.96	2.36		2.29
8	$[Fe(TMP)(N\text{-}MeIm)_2]ClO_4$	$^1/_2$	5225.61	5225.62	−0.35	505.76	506.22	−0.05	73.03	72.76	1.30	2.33	2.25	2.15
9	$[Fe(TMP)(N\text{-}MeIm)_2]ClO_4$	$^1/_2$	5225.61	5225.62	−0.35	505.76	506.22	−0.05	73.03	72.76	1.30	2.31	2.25	2.13
10	Fe(OEP)(NO)	$^1/_2$	5225.64	5225.65	−0.29	505.73	506.27	−0.01	72.89	72.54	0.94	2.35	2.18	2.10
11	Fe(OEP)(NO)	$^1/_2$	5225.64	5225.65	−0.30	505.73	506.27	−0.02	72.88	72.54	0.94	2.37	2.22	2.16
12	$K_3[Fe^{III}(CN)_6]$	$^1/_2$	5225.54	5225.55	−0.50	505.72	506.18	−0.12	73.02	72.75	1.28	2.95	2.86	3.38
13	Fe(TPP)	1	5225.69	5225.70	−0.19	505.57	506.46	0.00	72.82	72.30	0.62	2.33	1.86	1.76
14	$Fe^{VI}O_4^{2-}$	1	5225.47	5225.48	−0.63	505.53	506.36	−0.14	73.44	72.84	1.79	3.81	3.72	5.10
15	$[Fe(OEP)(3\text{-}Clpy)]ClO_4$	$^3/_2$	5225.63	5225.66	−0.30	505.34	506.61	−0.07	73.22	72.42	1.15	2.39	2.05	2.01
16	deoxymyoglobin 1BZP	2	5225.70	5225.74	−0.13	505.11	506.85	−0.06	72.98	71.91	0.40	1.96	1.73	1.26
17	deoxymyoglobin 1A6N	2	5225.71	5225.75	−0.13	505.11	506.85	−0.06	72.97	71.91	0.39	1.93	1.69	1.19
18	deoxyhemoglobin α	2	5225.70	5225.74	−0.15	505.09	506.85	−0.07	72.99	71.91	0.41	2.03	1.78	1.38
19	deoxyhemoglobin β	2	5225.70	5225.74	−0.13	505.10	506.86	−0.06	72.99	71.91	0.41	1.99	1.74	1.30
20	$KFe^{II}F_3$	2	5225.77	5225.81	0.00	505.12	506.90	0.00	72.78	71.71	0.00	1.28	1.14	0.00
21	Fe(TPP)Cl	$^5/_2$	5225.63	5225.68	−0.26	504.95	506.95	−0.12	73.44	72.15	1.10	2.18	2.04	1.79
22	metmyoglobin	$^5/_2$	5225.62	5225.67	−0.28	504.90	506.97	−0.15	73.50	72.17	1.18	2.25	2.02	1.84
23	Fe(TPP)Br	$^5/_2$	5225.64	5225.69	−0.26	504.96	506.95	−0.11	73.43	72.15	1.08	2.19	2.04	1.80
24	$Fe^{III}F_3$	$^5/_2$	5225.63	5225.68	−0.28	504.83	507.02	−0.17	73.55	72.12	1.18	1.92	1.85	1.34
	rmsd				0.14			0.05			0.39			1.02

[a] $\Delta\rho_i(0)$ (i = 1, 2, 3, val) are referenced to the data of $KFe^{II}F_3$.

configuration. Rather, our results imply that it is overwhelmingly the valence MO $\rho(0)$ values which change with chemistry and that the S values are relatively constant. This agrees well with a previous study[2] in which S was found to be relatively insensitive to orbital occupancy. Of course, it is possible that there *are* differences in S for different core orbitals, but if there are then they most likely do not vary with chemistry, since assumption of a uniform value already gives excellent results. In the future, it is possible that fully relativistic calculations might yield even further improved results, but a $\sim$0.07 mm s^{-1} rms error over the 2.34 mm s^{-1} range for 20 different systems appears to be a good start. In fact, it seems likely that uncertainties in crystallographic structures (especially in systems such as heme proteins), when combined with experimental uncertainties in δ_{Fe} measurement, may make further improvements quite difficult to obtain.

The observation that the core MO contributions are all relatively invariant to chemical bonding changes also helps explain the δ_{Fe} trends seen experimentally with changes in oxidation and spin state. For example, it is well-known that δ_{Fe} decreases with increasing oxidation state since there are fewer d electrons to shield the iron s electrons, so $\rho(0)$ increases. Thus, $Fe^{VI}O_4^{2-}$ has the smallest isomer shift, while Fe(II) systems such as deoxymyoglobin, deoxyhemoglobin, and $KFeF_3$ have

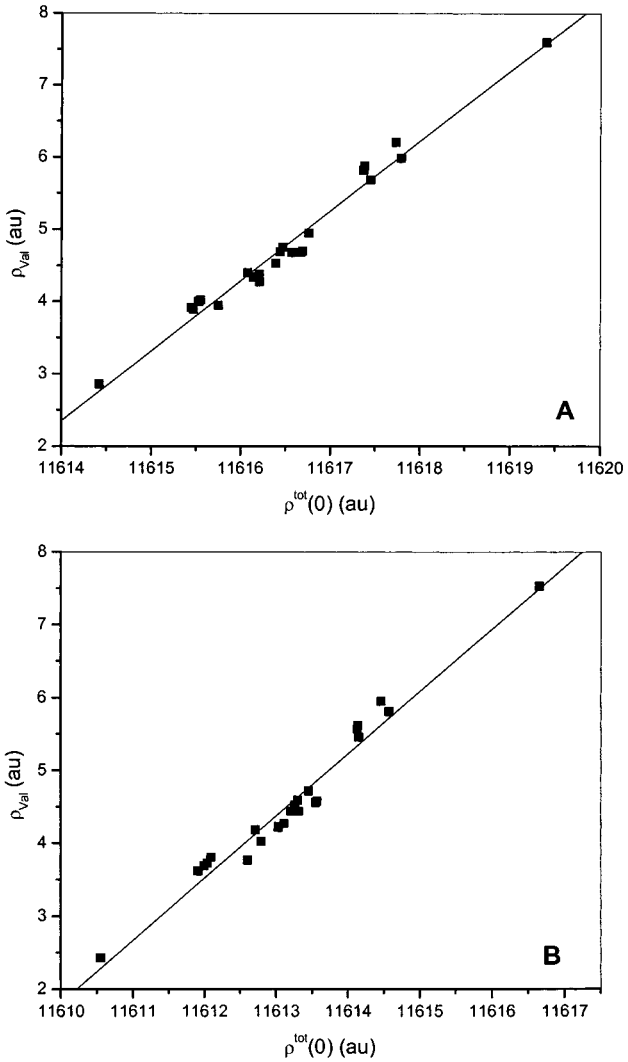

Figure 4. Graphs showing correlation between the total charge density at the nucleus ($\rho^{tot}(0)$) and the total valence shell charge density contribution. (A) BPW91 calculations and (B) B3LYP calculations. Data from Tables 6 and 7.

the largest isomer shifts, with most of the changes in $\rho(0)$ being located in the higher occupied MOs. In addition, there is also a clear effect of spin state on $\rho(0)$. For example, for Fe(II), δ_{Fe} increases in the order $S = 0, 1, 2$, while for Fe(III), δ_{Fe} increases in the order $S = {}^1/_2, {}^3/_2, {}^5/_2$. That is, δ_{Fe} increases with increasing spin state in both ferrous and ferric complexes, since usually the iron−ligand distances in high-spin compounds are larger than those in low-spin compounds, and this larger distance leads to a reduced electron density at the Fe nucleus, and hence an increased δ_{Fe}.

Finally, it is also of some interest to investigate in a more graphical manner the various MOs computed by using the DFT method, especially since, as we will show elsewhere, the computed wave functions also provide considerable data on spin density distributions (NMR hyperfine shifts[44] and ESR hyperfine coupling constants[45]), and it is of general interest to compare results on electronic structure obtained by using DFT methods with, e.g., ligand field approaches (which have been less successful in predicting, e.g., δ_{Fe} values[1]). By way of example,

(44) Mao, J.; Zhang, Y.; Oldfield, E., unpublished results.
(45) Gossman, B.; Zhang, Y.; Oldfield, E., unpublished results.

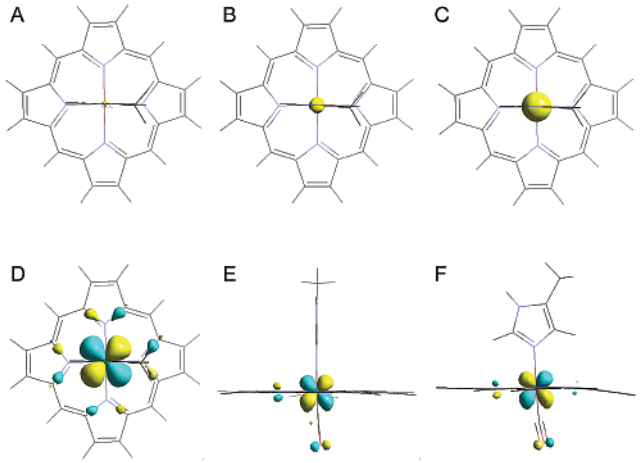

Figure 5. Molecular orbitals for carbonmonoxymyoglobin model system. (A−C) The three major MOs contributing to $\rho(0)$, the charge density at the iron nucleus (primarily the Fe 1s, 2s, and 3s orbitals). (D−F) The three major iron d-electron-containing MOs, $(d_{xz,yz})^4,(d_{xy})^2$. The contour values of these six MOs are all ±0.08 au.

we show in Figure 5 the three major MOs contributing to $\rho(0)$ for carbonmonoxymyoglobin, together with the three MOs containing the Fe d electrons. Clearly, we obtain the expected $(d_{xz},d_{yz})^4(d_{xy})^2$ configuration from ligand field theory. However, as emphasized by Debrunner,[1] ligand field methods do not readily enable the prediction of experimental δ_{Fe} values, while as demonstrated above, use of the hybrid DFT method and basis set scheme we have chosen does permit accurate prediction of δ_{Fe} values for a wide range of systems, making the iron-57 Mössbauer isomer shift an even more useful probe of geometric and electronic structure.

Conclusions

The results we have described above are of interest for a number of reasons. First, we have found that ^{57}Fe Mössbauer isomer shifts can be quite accurately predicted for a broad range of inorganic, organometallic, and metalloporphyrin/metalloprotein model compounds. The experimental range of δ_{Fe} values is 2.34 mm s^{-1}, while the rms deviation between calculation and experiment is only 0.080 mm s^{-1} (BPW91) or 0.067 mm s^{-1} (B3LYP), for systems containing d^2 to d^8 iron, and all spin states ($S = 0, {}^1/_2, 1, {}^3/_2, 2, {}^5/_2$) are quite accurately predicted. Second, we reproduce the "consensus" value of $\alpha^{rel} = -0.267 \pm 0.115\ a_0^3$ mm s^{-1} by using the HF method, a result which increases by only about 20% when using the DFT/B3LYP method, which also enables the prediction of other properties, such as the ^{57}Fe NMR chemical shift and the ^{57}Fe NMR chemical shift anisotropy, as well as NMR hyperfine shifts.[14,44] While several of the computational methods provide good linear correlations between experimental isomer shifts and theoretical charge densities at the iron nuclei, the derived α values vary considerably. However, the B3LYP functional provides good α, δ_{Fe} as well as other property values, so in most cases it appears to be the method of choice. Third, our results suggest that there are only minor changes in the core MO $\rho(0)$ values with changing chemistry, even though they contribute ≳99.9% to the overall charge density at the nucleus. The major changes in $\rho(0)$ with varying chemistry are due to higher occupied MOs or valence contributions. When taken together, these results indicate that use of the DFT method, especially incorporating

the B3LYP hybrid exchange-correlation functional, enables excellent predictions of ^{57}Fe Mössbauer isomer shifts, making this method a generally applicable one, even for complex paramagnetic metalloporphyrins and metalloproteins. In the future, it should therefore be possible to add the isomer shift to the list of properties which can be used to refine the local geometries of heme proteins, in much the same way that NMR, IR, and Mössbauer quadrupole splittings have been used already.[6]

Acknowledgment. This work was supported by the United States Public Health Service (NIH Grant EB-00271) and by the National Computational Science Alliance (Grants MCB-000018N, MCB-000020N, and MCB-010016N). We thank Dr. Friedrich Biegler-Koenig and Professor R. F. W. Bader for helpful advice and a copy of their AIM 2000 program, and the reviewers for valuable suggestions.

JA011583V